Available online at www.sciencedirect.com
ScienceDirect
Energy Reports 8 (2022) 381–391
www.elsevier.com/locate/egyr

2021 8th International Conference on Power and Energy Systems Engineering (CPESE 2021), 10–12 September 2021, Fukuoka, Japan

IEC 61850 modeling of an AGC dispatching scheme for mitigation of short-term power flow variations

Taha Selim Ustun[a,*], S.M. Suhail Hussain[a], Dai Orihara[a], Daisuke Iioka[b]

[a] *Fukushima Renewable Energy Institute, AIST (FREA), Koriyama, 963-0298, Japan*
[b] *Department of Electrical Engineering, Tohoku University, Sendai, Japan*

Received 26 October 2021; accepted 8 November 2021
Available online 27 November 2021

Abstract

High penetration of renewable energy-based generators increases variability in power systems. To prevent transmission lines from overloading due to such variations, advanced power flow management system should be developed. This paper proposes an Automatic Generation Control (AGC) design that mitigates power flow increase on heavy load lines. The developed method optimizes dispatching of control order from AGC so as not to increase power flow of these lines. This is achieved by considering how the output change of each control unit effects power flow in the system. The performance of the proposed method is examined by simulation study with 10-machine power system model. Furthermore, the communication infrastructure of the developed AGC system and its components are developed according to IEC 61850 communication standard. Operational instructions are mapped onto IEC 61850 messages. Simulations are performed with network emulators to validate the developed communication models and their operation. The benefit of the proposed communication system with IEC 61850 is achieving plug and play capability with universal models. The results of both simulations show that communication infrastructure is successfully developed and AGC prevents power flow increase in heavily loaded lines by making use of remained capacity of light loaded lines as proposed.

Peer-review under responsibility of the scientific committee of the 8th International Conference on Power and Energy Systems Engineering, CPESE, 2021.

Keywords: Power system communication; Smart grid; IEC 61850; MMS message; IEC 62351-4; Automatic Generation Control (AGC); Power flow control; Linear programming; Network emulation

1. Introduction

The penetration of renewable energy sources to electric power system is still expanding especially for photovoltaic and wind generation [1–3]. This emphasizes the importance of developing countermeasures for the problems caused by intermittency of the renewables [4–6]. Among all these different problems, this paper focuses on the increase of power flow variation. In conventional power system operation, short-term supply–demand balance is maintained

* Corresponding author.
E-mail address: selim.ustun@aist.go.jp (T.S. Ustun).

https://doi.org/10.1016/j.egyr.2021.11.153

Peer-review under responsibility of the scientific committee of the 8th International Conference on Power and Energy Systems Engineering, CPESE, 2021.

by secondary control such as Automatic Generation Control (AGC) and Load Frequency control (LFC). In [7], LFC performance defined by frequency stability and tie-line power flow stability is enhanced by using UPFC, IPFC and redox-flow battery. And [8] proposed the LFC system designed to suppress power flow fluctuations not only on tie-line but also on lines in the network. On the other hand, [9] proposed the AGC system that prevents transmission lines in the network from overloading by effectively using remaining capacities of light-loaded lines. This paper advances that work further so that AGC order dispatching is optimized dynamically depending on feedback information of the power flows. The performance of power flow variation mitigation is significantly improved because state of power flow can be considered in dispatching optimization at each control cycle. Although the power flow constraint on transmission lines is considered in the tertiary control, the high penetration of renewables brings injection of much of short-period power fluctuations, and the power flow constraint needs to be considered.

Most of the AGC and LFC schemes are designed assuming an interoperable, reliable and robust communication is present. Less research attention has been paid on developing standardized and interoperable communication for realizing AGC and LFC schemes. Considering that such schemes require different generators and grid components to communicate with each other, regardless of their models or manufacturers [10–12]. Therefore, achieving a standard language that all components can use is indispensable for real-life implementation of such control schemes [13–15].

In this regard, this paper proposes a holistic IEC 61850 communication based AGC order dispatching scheme. The IEC 61850 information models and information message exchanges between AGC, generators and Measurement Units (MUs) are developed for realizing the proposed AGC order dispatching scheme. The performance of the proposal is evaluated by time domain simulation with 10-machine system model representing two-area power system in east Japan. Furthermore, an emulation platform using IEC 61850 emulators and network simulators is developed to validate the IEC 61850 communication based AGC scheme and evaluate its performance in terms of End-to-End (ETE) delays.

2. Overview of automatic generation control and proposed control scheme

In steady state of power system, all Synchronous Generators (SGs) are almost synchronized. Their rotating frequency is equivalent to the system frequency, which is the controlled variable of AGC. Dynamics of SG is described by swing equation in (1).

$$M\frac{d\Delta f(t)}{dt} = P_m(t) - P_e(t) \tag{1}$$

Where, M denotes inertia constant, Δf denotes deviation of frequency from reference value, P_m denotes mechanical input and P_e denotes electrical output. P_e changes depending on load demand or the other power sources including renewables. To maintain frequency at reference value, P_m should be controlled to follow P_e. This frequency control is composed of primary, secondary, tertiary, and time control [16]. The primary control is known as Frequency Response (FR) and provided by speed governor and load characteristic. It responds to frequency fluctuation within a few seconds. The secondary control provided by AGC or Load Frequency Control (LFC) keeps frequency and tie line power flow at scheduled value by minute-to-minute balancing in controlled area. Time frame of the secondary control is 1–10 min. The tertiary and time control have longer time frame and keep long-term frequency stability.

In the conventional AGC, targets of power flow control function are only grid-tie lines. However, other lines of the power network should also be considered, as large penetration of renewables would bring large variation to all line power flows. Proposed AGC controls active power injected or absorbed by different components such as generation power plant, energy storage, controllable load, so that short term supply–demand balance is maintained. The power flow fluctuation depends on how the AGC control order is dispatched to those control units. Then, this paper proposes optimization method of AGC order dispatching for avoiding line overloads. Fig. 1 shows configuration of the proposed control system. The AGC block computes control order from the system frequency and tie line power flow, and the order is distributed to control units at specified ratio as (2).

$$S_{AGC,i} = k_i S_{AGC}\ (i = 1, \ldots, n_{AGC}) \tag{2}$$

where, S_{AGC} denotes control order of AGC, i denotes index number of AGC units,

The optimization scheme of the dispatching ratio has offline and online processes. At first, as the offline process, target lines are selected based on estimated power flow which is calculated from operation schedule of

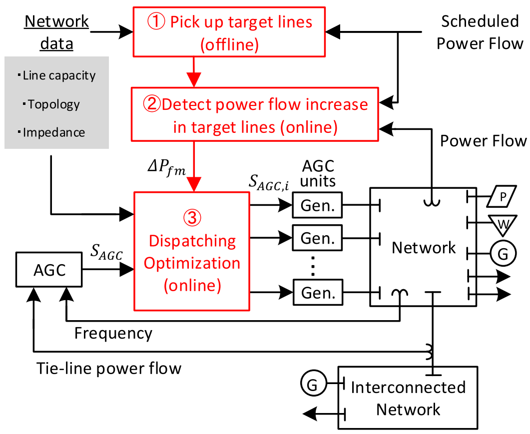

Fig. 1. AGC system with proposed order dispatching algorithm.

generation plants and forecasting of load demand and renewable generations. Threshold value of load factor is set and transmission lines with estimated load factor over the threshold value are picked up as target heavy load lines. The reason why heavy loaded lines are chosen as target is that those lines have low remaining capacity and will encounter issues with even small power flow increases. Next, as 1st step in online process, the power flows of target lines are monitored online. If a power increase is detected on the targets, the dispatching ratio is optimized so that the power increase is minimized in 2nd step in online process. While the power increase is not detected, dispatching ratio is set to be constant at generation capacity ratio. Here power increase means excess of power flow over estimated value.

The objective function of the optimization process is defined as minimization of maximum power flow increase among target lines at which power flow increase is detected as shown in (3).

$$\text{Objective minimize} \max_{\text{j}} \left[\Delta P_{fm,j}\left(t_s\right) + \Delta \hat{P}_{fc,j} \right] \tag{3}$$

where, j is index number of target transmission lines at which power flow increase is detected. ΔP_{fm} denotes detected power flow increase and $\Delta \hat{P}_{fc}$ denotes estimated power flow change made by AGC order implementation. t_s denotes certain sampling time. The constraints considered here are explained as below. The equality (4) means that the AGC order S_{AGC} must be dispatched to AGC units without any excess and shortage. The inequalities (5) and (6) mean that dispatching ratio k_i must be updated so that the assigned order for each unit does not violate ramp rate limitation and reserve capacity limitation, respectively.

Subject to

$$\sum_{i=1}^{n_{AGC}} k_i = 1 \tag{4}$$

$$\underline{r_i}\Delta t \leq S_{AGC,i}\left(t_s\right) - S_{AGC,i}\left(t_s - \Delta t\right) \leq \overline{r_i}\Delta t \tag{5}$$

$$\underline{b_i} \leq S_{AGC,i}\left(t_s\right) \leq \overline{b_i} \tag{6}$$

where, $\underline{r_i}$ and $\overline{r_i}$ denote minimum and maximum ramp rate of AGC unit #i. $\underline{b_i}$ and $\overline{b_i}$ denote lower and upper limit of reserve capacity that AGC unit #i have. Δt is sampling interval time.

The deterministic variables in the numerical programming are dispatching coefficients k_i. A relation between the coefficient and the estimated power flow change $\Delta \hat{P}_{fc}$ (MW) is described as (7), which is derived by applying DC power flow as power flow computation method.

$$\Delta P_{fc,j} = A_{ji} k_i S_{AGC} \tag{7}$$

where, $k_i S_{AGC}$ (MW) means injected active power from AGC unit #i and A_{ji} denotes relation between line power flow and nodal injection. A_{ji} is computed from network data which is topology and line impedances. Since the topology is not changed so often in high voltage transmission network, the coefficient A_{ji} is constant and does not need to be computed on-line. The advance from the method proposed in [9] is in the process of dispatching ratio computation. The old one does not have online process and computes the ratio in advance based on only day-ahead operation plan. While online measurement of power flow is not needed, power flows are always reduced even if power flow increase does not occur at the target lines.

3. Validation simulations and test results

Fig. 2 shows the power system model used for the simulation study. The model is developed based on 10-machine system model which represents the east area power system in Japan [17].

There are two area power systems, Area 1 and Area 2, which have single interconnection and their parameters are given in Table 1. In order to simulate a situation that large fluctuations are on transmission line power flow, three 2-GW wind generation systems are connected to the network as WG1, WG2 and WG3. The synchronous generators are modeled by swing equation shown in (8).

$$M\frac{d\Delta f_i}{dt} = P_{m0,i} + \Delta P_{m,i} - P_{e,i} - D\Delta f_i \tag{8}$$

where, P_{m0} (MW) denotes initial value of mechanical input and ΔP_m (MW) denotes its change given by frequency controller. D (MW/Hz) is damping coefficient. Wind turbine is modeled as a power source generating specified active and reactive power under an assumption that wind turbine is operated in Maximum Power Point Tracking (MPPT) mode and outputs in maximum independent on variation of frequency and voltage. Primary control and AGC are considered as frequency controller as shown in Fig. 3 which includes turbine models. The primary control is decentralized system and control order is computed by each generation unit from the rotating frequency of their mass as (9), where S_{GOV} (MW) is the control order and K_{GOV} (MW/Hz) denotes proportional gain.

$$S_{GOV,i} = -K_{GOV,i}\Delta f_i \tag{9}$$

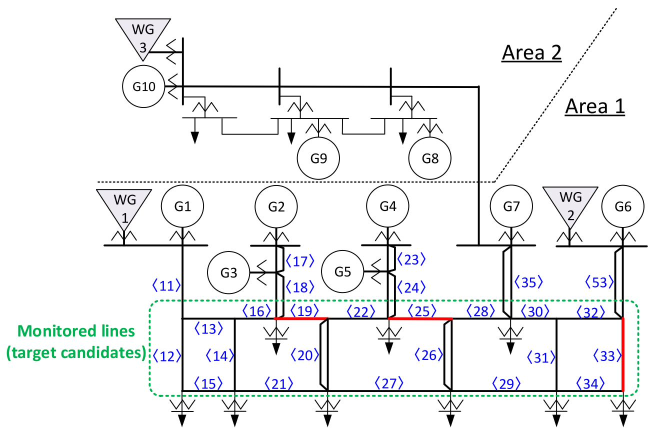

Fig. 2. Power system model used in validation studies [17]. (For interpretation of the references to color in this figure legend, the reader is referred to the web version of this article.)

On the other hand, AGC is centralized control and control order is computed by system operator such as TSO. AGC controller computes Area Control Error (ACE) as mismatch of supply and demand in target area firstly, and control order is computed so that ACE is converged to zero based on integral controller as (10), where K_{AGC} is integral gain [18].

$$S_{AGC}(s) = -(K_{AGC}/s)\, ACE(s) \tag{10}$$

Here, different types of AGC are assumed to be adopted in Area 1 and Area 2 according to actual system. The difference is in computation of ACE as shown in (11), (12).

$$ACE_1 = K_{B,1}\Delta f_{area,1} \tag{11}$$

$$ACE_2 = K_{B,2}\Delta f_{area,2} - \Delta P_{tie} \tag{12}$$

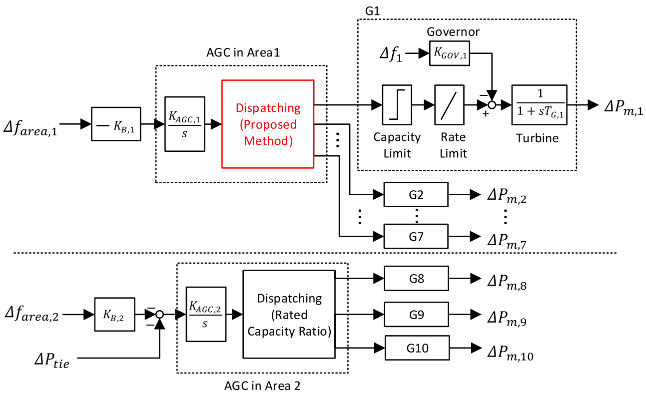

Fig. 3. Control system model for the proposed AGC Scheme.

Table 1. System parameters.

Parameter	Area 1	Area 2
System capacity (GVA)	60.0	15.5
System constant K_B (GW/Hz)	7.55	1.55
AGC integral gain K_{AGC} (1/s)	3.0×10^{-2}	3.0×10^{-2}
Governor gain K_{GOV} (puMW/Hz)*	0.25	0.25
Turbine time constant T_G (s)	10.0	10.0
AGC reserve capacity (puMW)	3.0×10^{-2}	3.0×10^{-2}
Maximum ramp rate (puMW/min)*	4.0×10^{-2}	4.0×10^{-2}

*Base value is rated capacity of each unit.

Table 2. Case settings.

Case	AGC order dispatching ratio	Target
Conventional	Ratio of rated capacities	N/A
Offline (>40)	Offline optimization [9]	Monitored lines, load factor > 40%
Proposed (All)	Proposed Scheme (Variable)	All monitored lines
Proposed (>40)	Proposed Scheme (Variable)	Monitored lines, load factor > 40%

where, K_B (MW/Hz) is system constant denoting relationship between imbalance power and frequency change, and Δf_{area} (Hz) denotes deviation of average frequency in each area. In this simulation study, center of inertia of frequency deviation is used as Δf_{area}. ΔP_{tie} (MW) is tie line power flow deviation from reference value. Control cycle of AGC is set to 3 s. The optimization process of the proposal starts after the AGC order is determined. Under our environment (RAM: 64 GB, Processor: Intel® Core™ i7-9700K 3.60 GHz), the optimization takes 0.18 s at most. The influence of the time delay of AGC order dispatching for the optimization calculation is expected to be quite small because it is corresponding to 6% of time cycle.

Initial load condition is assumed to be heavy (80%). Variation of load demand and wind generation are given as time series data. Uncertain short-term fluctuation is processed by filtering random data so as to have almost same variation characteristic as actual data. It is assumed that the proposal is applied to Area 1 and all units are controllable for AGC. Candidates of target for proposal are shown in Fig. 2 as "Monitored lines", which are all lines in Area 1 except connection line of power source such as #11, #12, #13, etc. This is because those connection lines have enough capacity for transmitting maximum output of the source.

In order to verify the effectiveness of the proposed scheme, a comparative study was carried out among four cases shown in Table 2. In the first case "Conventional", AGC order dispatching ratio is set to the ratio of rated capacities of AGC units to simulate conventional system dispatching rule. In the second case "Offline(over40)", dispatching ratio is optimized by offline method proposed in [9]. Targets are set to lines with load factor over 40% at initial state (line #19, #25 and #33 as shown in Fig. 2 by red color). In the third case "Proposed (All)", all candidates are set as target of the proposal. And last case "Proposed (Over40)" is the case in which targets are same as "Offline (over40)".

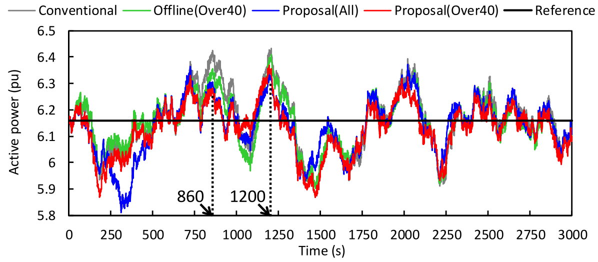

Fig. 4. Time variation of power flow of the target line #19.

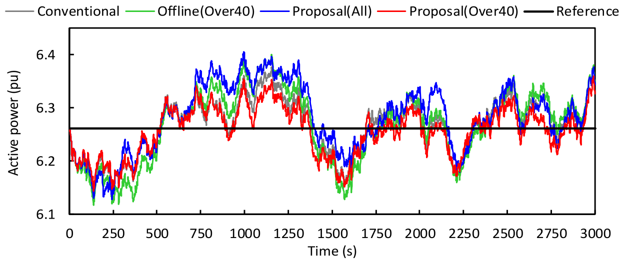

Fig. 5. Time variation of power flow of the target line #33.

Fig. 4 shows time variation of power flow of line #19 which is one of the targets. Initial power flow is 6.15MW and this is the reference value. The figure shows that the proposed method reduces large increase of the power flow at $t = 860$ s and $t = 1200$ s independent from target line selection. On the other hand, in "Offline (Over40)" case, reduction of maximum power flow is smaller than that in "Proposed (Over40)" case. Since offline method determines dispatching ratio so that power flow is always decreased at all target lines, it is difficult to give great contribution on only a part of targets even if large increase occur at those lines. The result of another target line #33 is shown in Fig. 5. Different from the line #19, maximum power flow has been increased in "Proposed (All)" case and "Offline (Over40)" case while the reduction of maximum power flow can be seen in "Proposed (Over40)" case.

In order to evaluate the effect of the proposed method for all lines quantitatively, reduction ratio of maximum deviation of power flow from reference value is computed for all lines. Fig. 6 shows the computation results. Positive value means that the maximum deviation is reduced by the proposed control scheme, likewise, the negative value means increase of maximum power flow. In 'Proposed (All)' case, maximum power flow increases at 7 lines (#33, #12, #13, #14, #28, #31, #32) in 19 targets. On the other hand, focused on heavy load lines as 'Proposed (Over40)' case, maximum power flow can be reduced for all targets (#19, #25, #33). The more transmission lines are set to target, the performance is deteriorated because the combination of dispatched generation units effective to reduce maximum power flow of target lines decreases. Compared 'Proposed (Over40)' case with 'Offline (Over40)' case, it is found that the performance is significantly improved especially at target line #33(-17.0% to $+16.3\%$ as shown in Fog. 6)). Since the proposed scheme optimizes AGC order dispatching considering how much the power flow increases at each target line every control step, maximum power flow can be decreased effectively.

Although the proposed method does not consider power flow change at non-target lines, there are some lines at which power flow increases largely as line #12, and there is possibility that overloading occurs at non-target line. It is a challenge to be addressed in further research to consider load factor of non-target line in the dispatching optimization.

Since the proposed method controls AGC order dispatching, AGC performance is expected to be affected. Table 3 shows standard deviation (STD) of ACEs in both areas. It is found that the proposed method increases STD of ACE_1 especially in 'Proposed (Over40)' case. When a smaller group of lines is picked up as target, less AGC units which have high sensitivity to target line power flow tend to be mainly used. Since the number of units that the control order is dispatched effects how fast the total AGC unit output follows to the control order, reduction of number of dispatched units causes deterioration of frequency regulation performance. On the other hand, it is also found that AGC performance in Area 2 is not affected so much if the proposal is applied to Area 1.

Table 3. Standard deviation of frequency control performance.

Case	STD of ACE_1 (MW)	STD of ACE_2 (MW)
Conventional	259	154
Offline (over 40)	260(+0.4%)	157(+1.9%)
Proposed (All)	260(+0.4%)	154(±0.0%)
Proposed (over 40)	280(+8.1%)	156(+1.3%)

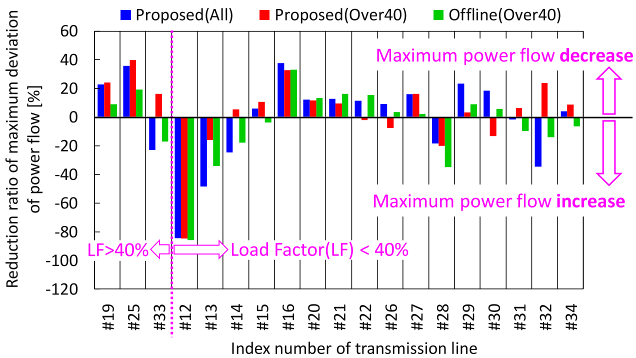

Fig. 6. Reduction ratio of maximum power flow of all candidate lines.

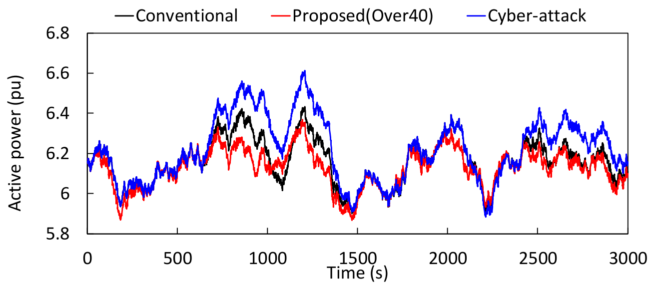

Fig. 7. Time variance of power flow of line #33 which is one of the targets of proposed method.

In 'Proposed (Over40)' case, polarity of power flow data transmitted from measurement point to AGC controller is reversed to simulate cyber-attack. In such a situation, the proposed method optimizes AGC order dispatching ratio so that maximum power flow at target lines is increased as possible. As shown in Fig. 7, the power flow of target line #33 varies largely. The result shows importance of developing secure communication scheme as shown in following section.

4. IEC 61850 based secure communication design for proposed dispatching scheme

As presented above, the proposed AGC dispatching schemes requires constant information exchange between different components in the power network. Not only do they belong to different manufacturers but also different domains, e.g. generators, measurement units and electronic controllers. This requires a mutually comprehensible language.

The communication for the proposed AGC dispatching scheme is designed according to IEC 61850. The communication model for generators is developed according to the IEC 61850 information model using the logical nodes defined in IEC 61850-7-420 standard [19]. IEC 61850-7-420 information model for the generators is shown in Fig. 8. The logical nodes (LNs) DRCC and DSCH in the generator communication model are utilized for receiving the data related to dispatch from the AGC. The '*OutWSet*' data object (DO) in LN DRCC is utilized to specify dispatch value i.e. active power. The DO '*SchdVal*' in DSCH is used to identify the type of dispatch as defined

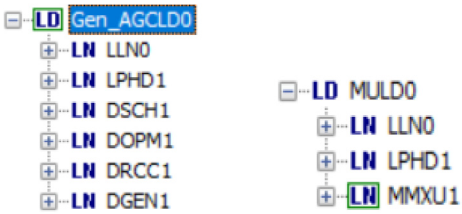

Fig. 8. IEC 61850 information model for generators and MUs.

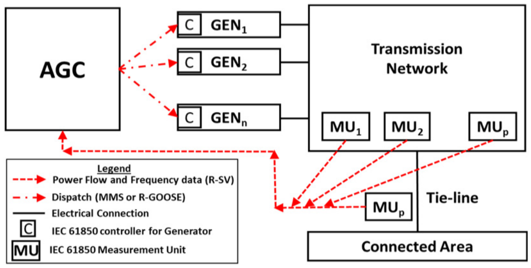

Fig. 9. IEC 61850 communication model for AGC dispatching scheme.

by IEC 61850-7-420 standards. For example, a value of 1 in DO '*SchdVal*' corresponds to active power dispatch, while 2 corresponds to reactive power dispatch.

Similarly, the MUs are modeled with MMXU LNs. The MMXU LN contains DOs '*TotW*', '*TotVAr*' and '*Hz*' which corresponds to active power, reactive powers and frequency measurements, respectively. Fig. 8 shows the information model of MU.

The MUs placed on all the power lines in transmission network. These MUs communicate the measured values (i.e. active power, reactive power and frequency) of each transmission line to the *AGC_Controller* in control center as shown in (13). Where p denotes number of MUs in the system. MUs communicate this information by publishing Routable Sample Value (R-SV) multicast messages. And *AGC_Controller* subscribes to these R-SV messages. The size of R-SV message with '*TotW*', '*TotVAr*' and '*Hz*' along with headers data is calculated as 160 bytes.

$$MU_p\_MMXU_p.(TotW\,\&\,TotVAr\,\&\,Hz).MV \rightarrow AGC\_Controller \tag{13}$$

Based on these measurements the *AGC_Controller* calculates the dispatch values for each generator as (2) described in Section 2. The dispatch values are communicated to the respective controllers of the generators through IEC 61850 Manufacturing Message Specification (MMS) write request–response messages. As shown in Fig. 9, these messages carry very critical information and need to be secured against cyberattacks. In line with IEC 62351 cybersecurity standard that secures IEC 61850 messages, they are exchanged over a secure Transport Layer Security (TLS) connection. This means the messages are both encrypted and hashed to mitigate unauthorized viewing and editing, respectively. This information flow is shown in (14) and (15). Fig. 9 depicts the communication design for the proposed AGC dispatching scheme.

$$AGC\_Controller \rightarrow GEN_n\_DSCH_n.SchdVal\,\$\,ING = 1 \tag{14}$$

$$AGC\_Controller \rightarrow GEN_n\_DRCC_n.OutWSet\,\$\,APC \tag{15}$$

5. Performance evaluation of communication design

In order to demonstrate the IEC 61850 communication based AGC dispatching scheme and evaluate its performance in terms of End-to-End (ETE) delays, a network emulation platform shown in Fig. 10 is developed. The wide area communication network of east area power system of Japan, shown in Fig. 2, is modeled in network simulator tool [20]. In emulation tests, the nodes representing generators, MUs and *AGC_Controller* are placed such that the distance among them is approximately same as the east area power system of Japan.

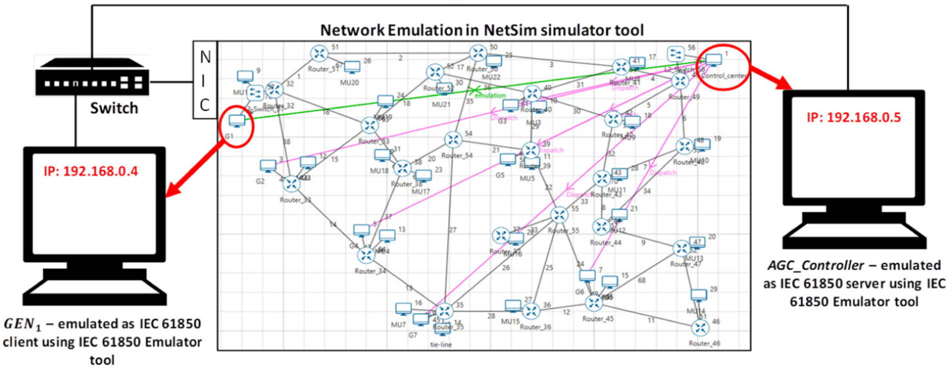

Fig. 10. Laboratory emulation platform set up .

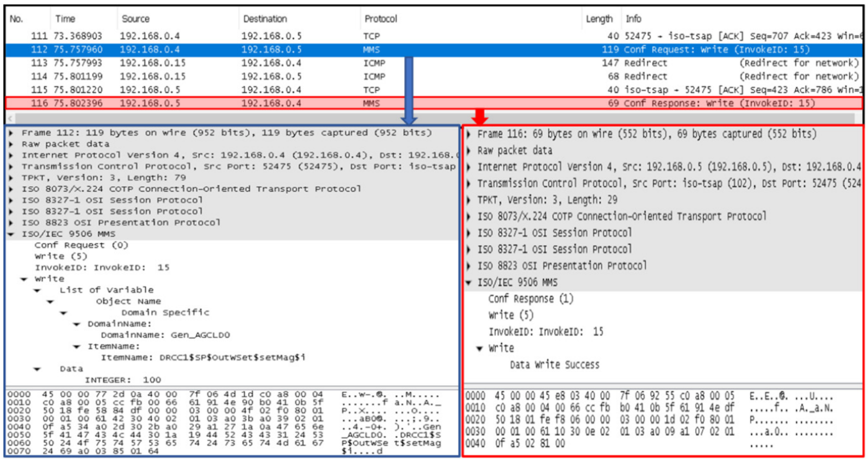

Fig. 11. IEC 61850 MMS write request–response message for dispatch order exchanged between AGC_Controller and GEN1.

The generator 1 (GEN_1) and *AGC_Controller* of test system (east area power system of Japan) are emulated using the IEC 61850 emulation tool on two separate PCs. The IED Capability Description (ICD) file developed from the information model, shown in Fig. 8, is used to emulate the GEN_1 and *AGC_Controller*. These emulated nodes GEN_1 (IP: 192.168.0.4) and *AGC_Controller* (IP: 192.168.0.5) act as IEC 61850 client and server, respectively, and exchange messages in real-time. GEN_1 and *AGC_Controller* are connected to '*G1*' and '*control_center*' nodes inside emulation platform, such that all the traffic generated by these nodes enters the simulation through '*G1*' and '*control_center'* nodes, respectively. Inside the simulation, the '*G1*' and '*control_center*' nodes are mapped to IP address '192.168.0.4' and '192.168.0.5' respectively, hence they receive all the external real traffic of IP address they are mapped with. This way, the real messages generated by emulated IEC 61850 client and server enter the simulation. These real messages pass through different routers, switches and communication links inside emulation tests experiencing the delays and packet losses before reaching the destination.

After setting up the emulation platform, the message exchanges required for realizing the proposed AGC dispatching scheme, as described in (13)–(15), are set in emulation test using application profile. All the 'MU_p' nodes in simulation are configured to multicast UDP messages (i.e. R-SV) of 160 bytes. The '*control_center*' node in simulation is configured to send two client–server messages of 119 and 117 bytes to all the '*Gn*' nodes. In addition to this simulated traffic, the *AGC_Controller* is configured to send two MMS write request–response message to GEN_1. These real messages generated from *AGC_Controller* enter the simulation via '*control_center*' node and pass through different routers, switches and '*G1*' node before reaching GEN_1. Figs. 11 and 12 show the Wireshark capture of MMS write request–response messages (representing (14) and (15)) exchanged between *AGC_Controller* and GEN_1. The successful exchange of IEC 61850 MMS messages validate the IEC 61850 information model

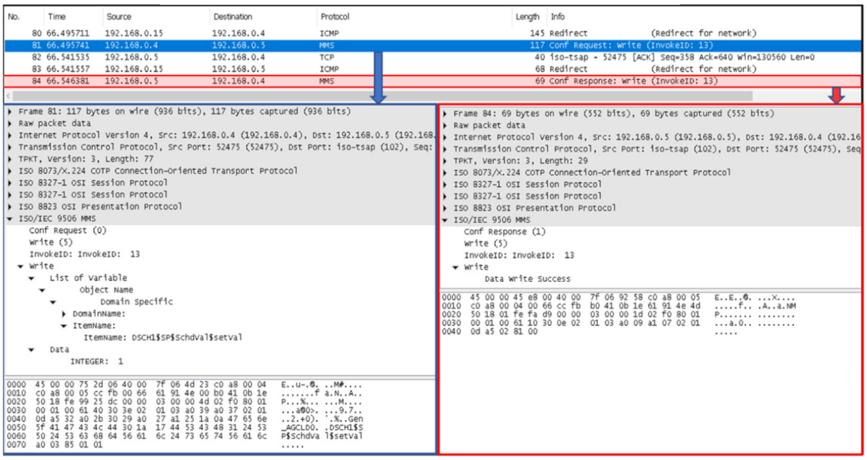

Fig. 12. IEC 61850 MMS write request–response message for dispatch schedule type exchanged between AGC_Controller and GEN1.

Table 4. ETE delay for IEC 61850 message exchanges.

Packet type	Information exchange	Message type	Message size	Average ETE in ms
Real	AGC_Controller → GEN_1	MMS	119	12
Real	AGC_Controller → GEN_1	MMS	117	12
Simulated	Control_center → Gn	MMS	119	10.8
Simulated	Control_center → Gn	MMS	117	10.8
Simulated	MUp → Control_center	R-SV	160	16

developed for the proposed AGC dispatching scheme. For legibility, unsecured messages captures are presented here. Detailed discussion on IEC 61850 MMS security is out of scope and can be found in [21].

The average ETE delays experienced by these real MMS messages inside simulation is given in Table 4. Further, the ETE delays obtained for MMS message exchanges between AGC (‘*control_center*’) and other generators (‘*Gn*’) inside simulation are given in Table 4. It also lists the average ETE delays obtained for exchanging R-SV messages between Mus and AGC. The ETE delays for all the messages are well within the limit of 100 ms required for AGC or LFC [22].

6. Conclusions

As the renewable energy penetration increases in power systems, power flow variation in transmission lines becomes more prevalent. This paper proposes a novel AGC design which has an additional function to avoid overloading of transmission lines in network. In the proposed system, dispatching of AGC order is optimized online by considering how the control unit output change effects the power flows. Simulation study on a 10-machine system model shows that the proposed method is effective to reduce power flow increase at heavy-loaded lines while the performance of AGC on regulation of frequency and tie-line power flow is slightly deteriorated. It is also found that the proposed method could not perform well if all lines are set to target because the proposal is designed to make use of remaining capacity of non-target lines. Optimization of target selection is one of the important challenges needed to be addressed in the future as well as coordination with energy storage and distributed generation.

A fully standardized communication model has been developed based on IEC 61850. The operation and message exchanges or the proposed AGC have been mapped onto IEC 61850 information models and message structures. The validation tests show that the messages can be successfully sent over long distances and ETE is acceptable for AGC operation time windows. These results are very valuable as they give realistic timing values and their applicability.

This work contributes to the main body of knowledge by developing standardized models for smart grid components and implementing a full scheme based on them. This is a solid step towards plug-and-play in power systems.

Declaration of competing interest

The authors declare that they have no known competing financial interests or personal relationships that could have appeared to influence the work reported in this paper.

References

[1] Hubble AH, Ustun TS. Scaling renewable energy based microgrids in underserved communities: Latin America, South Asia, and Sub-Saharan Africa. In: 2016 IEEE PES PowerAfrica, Livingstone. 2016, p. 134–8.
[2] Hubble AH, Ustun TS. Feasibility of microgrid optimization and grid extension for rural electrification. In: 2016 IEEE region 10 conference, 2016. p. 1266–9.
[3] Nkiriki J, Ustun TS. Mini-grid policy directions for decentralized smart energy models in Sub-Saharan Africa.In: 2017 IEEE PES innovative smart grid technologies conference Europe, 2017, pp. 1–6.
[4] Ustun TS, Aoto Y. Analysis of smart inverter's impact on the distribution network operation. In: IEEE access, Vol. 7. 2019, p. 9790–804.
[5] Hashimoto J, Ustun T, Otani K. Smart inverter functionality testing for battery energy storage systems. Smart Grid Renew Energy 2017;8:337–50. http://dx.doi.org/10.4236/sgre.2017.811022.
[6] Kikusato H, et al. Microgrid controller testing using power hardware-in-the-loop. Energies 2020;13(8):2044.
[7] El Yakine Kouba N, Menaa M, Hasni M, Boudour M. Frequency stability enhancement in two-area deregulated power system based competitive electricity markets with redox flow batteries and power flow controllers. In: Proc. 2016 8th int. conf. model. identif. control., 2017. p. 1029–36.
[8] Fukuda R, Kato M. AR allocation method to minimize power flow fluctuation by battery control. In: 2011 The international conference on electrical engineering, 2011.
[9] Orihara D, Iioka D. Sensitivity-based AGC dispatching for mitigation of short-term power flow variation. In: Conf. rec. 3rd IEEE int. work. electron. power grid, 2018. p. 1–6.
[10] Ustun TS. Design and development of a communication-assisted microgrid protection system [Thesis], Melbourne, Australia: Victoria University; 2013.
[11] Nadeem F, Aftab MA, Hussain SMS, Ali I, Tiwari PK, Goswami AK, et al. Virtual power plant management in smart grids with XMPP based IEC 61850 communication. Energies 2019;12(12):2398.
[12] Ustun TS. Interoperability and interchangeability for microgrid protection systems using IEC 61850 standard. In: 2016 IEEE international conference on power and energy, 2016. p. 7–12.
[13] Aftab MA, et al. IEC 61850 Communication assisted synchronization strategy for microgrids. In: 2018 IEEE 13th international conference on industrial and information systems, 2018. p. 401–6.
[14] Ustun TS, Hussain SMS, Kikusato H. IEC 61850-based communication modeling of EV charge-discharge management for maximum PV generation. In: IEEE access, Vol. 7. 2019, p. 4219–31.
[15] Farooq SM, et al. Certificate based security mechanisms in vehicular ad-hoc networks based on IEC 61850 and IEEE wave standards. Electronics 2019;8(1):96.
[16] NERC Resources Subcommittee. Balancing and frequency control. 2011, p. 11–4.
[17] IEEJ. IEEJ EAST 10-machine system model (50Hz). Available: http://denki.iee.jp/pes/?page_id=496.
[18] Kundur Prabha. Power System Stability and Control. New York: McGraw-Hill; 1994, p. 581–623.
[19] Communication networks and systems for power utility automation - Part 7-420: basic communication structure - distributed energy resources logical nodes. 1.0. IEC 61850-7-420,, IEC; 2009.
[20] Ustun TS. A critical review of IEC 61850 testing tools. Sustainability 2021;13(11):6213.
[21] Ustun TS, Hussain SMS. IEC 62351-4 security implementations for IEC 61850 MMS messages. In: IEEE access, Vol. 8. 2020, p. 123979–85. http://dx.doi.org/10.1109/ACCESS.2020.3001926.
[22] Communication Networks and Systems for Power Utility Automation - Part 90-5: Use of IEC 61850 To Transmit Synchrophasor Information According To IEEE C37.118. 1.0. IEC 61850-90-5,, IEC; 2012.